Chinese Chemical Letters 33 (2022) 1963–1969

Contents lists available at ScienceDirect

Chinese Chemical Letters

journal homepage: www.elsevier.com/locate/cclet

In situ wound sprayable double-network hydrogel: Preparation and characterization

Chenglong Cai[a,b,1], Ting Wang[a,b,1,*], Xu Han[a], Shaoqiang Yang[c], Chengteng Lai[c], Tao Yuan[c,*], Zhangqi Feng[d], Nongyue He[a]

[a] State Key Laboratory of Bioelectronics, National Demonstration Centre for Experimental Biomedical Engineering Education, School of Biological Science and Medical Engineering, Southeast University, Nanjing 210096, China
[b] Southeast University Jiangbei New Area Innovation Institute, Nanjing 210096, China
[c] Nanjing Jinling Hosp, Dept Orthoped, Nanjing 210002, China
[d] School of Chemical Engineering, Nanjing University of Science and Technology, Nanjing 210094, China

ARTICLE INFO

Article history:
Received 26 July 2021
Revised 13 November 2021
Accepted 15 November 2021
Available online 19 November 2021

Keywords:
Hydrogel
Sodium alginate
Chitosan
Spray method
Sodium carboxymethyl cellulose

ABSTRACT

In clinical settings the wound-dressing was required easy to use and can match the wound area immediately, at the same time they need to have the properties of hemostats, anti-inflammation and promoting wound healing. To get an ideal wound dressing, we developed a type of gel-like wound adhesive patch from spraying double-network hydrogel, which own the properties of self-antibacterial and can promote wound healing. By spraying, the gel-like wound adhesive patch can match the wound area immediately and form a gel-film in 10 s. Sodium carboxymethyl cellulose as pH sensitive materials accelerated the speed to form the gel-film and enhanced ductility of the wound adhesive patch. *In vitro* experiments show that, this gel-like wound adhesive patch can promote cell proliferation and reduce cell apoptosis. *In vivo* studies show that, compared with commercialized wound dressings in clinic using, the spraying gel-like wound adhesive patch from our work has a better effect on wound healing. In conclusion, the spraying gel-like wound patch in our work is easy to use and can form a gel-film match on wound area in a short time, also it has the properties of hemostats, anti-inflammation and promoting wound healing. Its feasibility for mass production shows a good potential for commercial use.

Wound dress in clinical settings is currently to protect exposed tissue, and mitigate bleeding, infection and inflammation [1]. To get an idea wound dressing, numerous natural polymers materials have been developed [2–4]. Double-network hydrogel from natural polymers is choosing for the latest generation. This type of hydrogel is considered can develop a type of gel-like wound adhesive patch with rapid film formation and adhesive on the wound area, also it can prevent bacterial invasion and promoting wound healing.

With the continuous upgrading of medical products, wound dressings have gradually changed from traditional dressing such as gauze bandage to new dressing such as ointment and gel [2]. Among them, hydrogels have been widely recognized in the society due to their excellent adhesion and water absorption characteristics. However, the preparation of raw materials with high molecular weight hydrogels requires many resources to be used to increase economic burden in preparation, packaging and transportation. Low molecular weight raw materials are simple and convenient for transportation, yet hydrogel membranes with mechanical strength cannot be constructed. The dual network hydrogel can solve this problem. The double-network hydrogel can compensate for the deficiency of heterogeneity of polymer network structure and avoided the poor mechanical stability of hydrogels. There are various types of double-network hydrogels, to form adhesive films rapidly on the wound surface based on natural polymer hydrogel. To improve the mechanical stability of gel-film, the double-network hydrogel was studied and developed to be a tough hydrogel with high strength [5]. Double-network hydrogel consists of two crosslinked networks with diverse physical properties. The first network has the characteristics of hard and brittle, the second network has soft and excellent ductility. The two networks can improve the mechanical properties of hydrogels together. In the structures of dual network hydrogel, the first network acts as a "sacrificial bond" in the process of gel deformation to play the role of dissipative energy, and the broken fragments form a "junc-

* Corresponding authors.
E-mail addresses: tingwang@seu.edu.cn (T. Wang), yuant1205@163.com (T. Yuan).
[1] These authors contributed equally to this work

https://doi.org/10.1016/j.cclet.2021.11.047
1001-8417/

tion point" in the second network [6]. It was considered that the double-network can maintain the integrity of the gel and contributes to the extensibility of the hydrogel during deformation. The double-network hydrogel can make up for the deficiency of heterogeneity of polymer network structure and avoid the poor mechanical stability of hydrogels. It was considered to be a good choice for wound dress. As it was statistics the associated annual global market is rapidly increasing with a growth rate of 9.7% and is expected to exceed 15 billion US dollars by 2024, based on simple and fast way to be use, sprayed hydrogel is charming for their commercialization [7,8].

Chitosan and sodium alginate were considered as good natural polymers to form double-network hydrogels, which have good biocompatibility and have broad commercial prospects in the field of wound dressing [9]. Chitosan is mainly composed of a range of presumably pure poly-β-1,4-*N*-acety-D-glucosamine materials whose properties are highly dependent on its degree of deacetylation [10]. Due to its reactive amino groups, the chitosan exhibits excellent biocompatibility, low toxicity and immune-stimulatory activities for applied in biological material [11]. However, the low solubility of chitosan and the high viscosity of the solution result in the brittle and weak physical network of the resulting chitosan, which cannot meet the physical needs of the first network of hydrogel [10]. To enhance antibacterial properties and improve the strength of hydrogels of chitosan, some of the works mixed nanoparticles into chitosan solution, some other works modified chitosan by succinic anhydride [11,12]. To enhance mechanical property of chitosan physical network is still difficult to be applied to the construction of double-network hydrogels.

Alginate is often used as a synthetic drug carrier, food processing and dressing material for diabetic wound ulceration basing on its excellent biocompatibility. However, the strength of alginate hydrogel is weak, and its young modulus unable to match with the tissue modulus. It is easy to cause the collapse of gel structure due to swelling. To developing sodium alginate hydrogel, electrospinning technology were used to build sodium alginate and wrapped with chitosan for wound closure [13], carboxymethyl cellulose were also used for preparing hydrogel materials [14]. But the complex processes lead to higher cost and less commercial promotion for double-network hydrogels from nature polymer. In this research, we developed a type of hydrogels by one-step spraying of short chain chitosan composite hydrogel to sodium alginate as a simple, fast and convenient method to form double-network hydrogel with high strength and toughness double-network. We successfully introduced chitosan crystallization, chain entanglement and ionic physical network into sodium alginate network and constructed a type of nature polymer based double-network hydrogel.

This type of skin regenerative double-network hydrogel is show up rapid film formation, antibacterial and biocompatibility. It is mainly composed of sodium alginate chelated with calcium ion and polymerized with chitosan, and a stable three-dimensional structure is formed by using the pH sensitive property of sodium carboxymethyl cellulose. The hydrogel rapidly polymerized in 10 s and had good adhesion to various wounds. This hydrogel material is widely distributed and easy to obtain. It can form a physical barrier to prevent microbial invasion. The results show that the hydrogel has broad market prospects.

This kind of skin regeneration dual network hydrogel has a young modulus similar to that of skin [15]. At the same time, sodium alginate with good hemostatic and analgesic properties was used as the first layer of weak alkali gel dressing, then sprayed a layer of acidic chitosan with antibacterial properties to form a stable three-dimensional structure by double-network cross-linking and pH sensitivity of sodium carboxymethyl cellulose [16,17]. The hydrogel rapidly polymerized in 10 s and had good adhesion to various wounds. This hydrogel is widely distributed and easy to obtain. It can form a physical barrier to prevent microbial invasion. The results show that the hydrogel has broad market prospects.

Sodium alginate was purchased from Aladdin Industrial Co. (Shanghai, China); sodium carboxymethyl cellulose (CMC) was obtained from Nanjing Chemistry Co., Ltd.; chitosan was purchased from Beijing Bailingwei Technology Co., Ltd. The acetic acid (CH_3COOH), sodium bicarbonate ($NaHCO_3$), alcohol and calcium chloride were obtained from Sinopharm Chemical Reagent Co., Ltd. All reagents are analytical pure.

The sprayed hydrogel consists from two kinds of solutions. One composed with sodium alginate and sodium carboxymethyl cellulose with the name of SC. The solution was under magnetic stirring at 60 °C until it becoming clear and uniform. The solutions without sodium alginate or without sodium carboxymethyl cellulose were named as CMC and SA. The other solution was prepared by acetic acid solution, chitosan, $CaCl_2$ and ethanol named CaCS. The preparation process of hydrogel membrane was to spray the two types of solution on to the surface of substrates. Hydrogel membrane will be formed in the first 10 s, which were named SCC hydrogel. The simple sprayed material like SA or CMC with CaCS material to forming hydrogel, we named SA/CaCS hydrogel or CMC/CaCS hydrogel.

The Fourier transform infra-red (FT-IR, Nicolet is 50 Thermo) was used for studying functional group in hydrogel with the wavenumber from 500 cm^{-1} to 4000 cm^{-1}. Samples used for FT-IR analysis was dried at 120 °C about 30 min and mixed with pellets with KBr.

The morphologies of SC, CaCS and SCC hydrogel were observed by scanning electron microscope (SEM, Ultra Plus Zeiss).

All rheological measurements were performed on MCR302 rheometer (Anton Paar) using a 40-mm parallel plate and a 1-mm gap distance at 15 °C. In order to test completely reactive gel materials, the solution was mixed and reacted 5 min for testing to ensuring each sample was analyzed under comparable condition.

We analyzed levels of skin sensitive, skin moisture, sebum, pigmentation and wrinkle with instruments of Courage + Khazaka electronic GmbH. 10 healthy volunteers were divided into 2 groups and all wolunteers below 35 years of age ($n = 10$, age $= 30.1 \pm 6.7$) were included in the study after providing informed consent. Age-weighted-average is compared with the database from the software with GmbH. Four skin windows (each 5 cm × 5 cm, surface area 25 cm^2) on the volar sides of both forearms of each volunteer were treated or served as control. Experiment group treated with hydrogel for 15 min with the name of "After", and before treatment the group was named with "before". All human studies were approved by the Ethics Committee of Najing Jinling Hospital (SCB108–206) and volunteers (Appendix informed consent.).

The antibacterial activity of three types of hydrogels was evaluated using *E. coli*., which were first incubated overnight in Mueller-Hinton Broth (MHB) at 37 °C with shaking, and then were diluted in MHB to a concentration of 106 colony-forming unit (CFU)/mL. Subsequently, 100 μL of the bacterial solution was seeded onto the agar surface. Agar was sprayed with SCC hydrogel (experiment group) or coat with commercialized wound dressing (control group). 1 mL of SCC hydrogel and agar were added to the culture dish as experiment group and control group. Bacterial dish was incubated at 37 °C for 24 h, and the number of bacterial colonies was recorded. Experiments were performed three times in each group. At the same time, PI staining were used for distinguish the living and dead baterials, then observed by confocal fluorescence microscope (Laica SP8).

The *in vitro* cytotoxicity of hydrogels was quantitatively determined by apoptosis assays. Hydrogels were prepared as substrate of the dish and ultraviolet (UV) sterilized for 1 h. C6 cells at a concentration of 3×10^3 cells per well were added into 96-well cul-

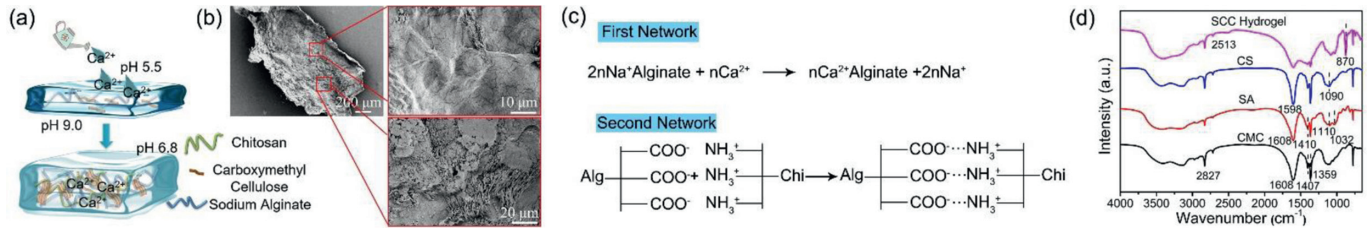

Fig. 1. (a) Schematic illustration of cartoon for hydrogel structure and formation process; (b) SEM of SCC hydrogel membrane and microstructure of hydrogel surface film; (c) Schematic illustration of formula for forming hydrogel network; (d) The FT-IR spectra of CMC, SA, CS and SCC hydrogel.

ture plates and incubated overnight. Following culture for an additional 24, 48, or 72 h, cell viability was evaluated *via* flow cytometry analysis. The biocompatibility of hydrogels was assessed through fluorescence microscopy observations of C6 cells. Hydrogels were seeded into 24-well plates and ultraviolet (UV) sterilized for 1 h. C6 cells (2×10^4 cells per well) were seeded on the surface of the UV-sterilized hydrogels. After culturing for 24, 48, or 72 h, cell proliferation assays were performed using Calcein-AM/PI Double Staining Kits. Images were obtained with a confocal fluorescence microscope (Laica SP8). Control cells were seeded into wells lacking hydrogels.

The wound healing capacities of hydrogel were evaluated using a rat model. White female rats, aged 6–8 weeks were opened pore with diameter of 20 mm on the back by punch. Before opened pore, the dorsal hair of rats was shaved by an electric shaver the skin disinfected using sterile normal saline and 70% ethanol. Then SCC was sprayed to the wound area as the experimental group. And the others were treated with market products, which were considered as control group. The wound area was measured by ImageJ software to trace the wound margin, and the unclosed wound rate was calculated as follows (Eq. 1):

$$\text{Unclosed wound rate } (\%) = A_t/A_0 \times 100\% \quad (1)$$

where A_0 is the initial wound area and A_t is the wound area at day t.

The rats were anesthetized on the 21st day after the opening. The whole skin around the wound was dissected, washed with normal saline, and fixed in 4% phosphate buffered polyoxymethylene solution. The sections were fixed on glass slides and stained with hematoxylin eosin (H & E) reagent for histological analysis. All the animal studies were approved by the Ethics committee of Najing Jinling Hospital (SCB108–206).

The pH value of SC and CaCS solutions were 9.0 and 5.5 by pH indicator strips before the two different solutions were loaded into sprinkling in Figs. 1a and b demonstrated the synthetic process of hydrogel. In order to further explore the surface morphology of SCC hydrogel membrane, we observed the surface of freeze-dried membrane by SEM showing in Fig. 1b. It was clearly observed that the thickness of hydrogel film was uniform, but the surface structure was complex. Two different type structures fill the whole membrane surface. Large number of fusiform structures can be found on the membrane surface as shown in the image which was amplified locally at bottom right, so we considered that should be sodium carboxymethyl cellulose. At the same time, chapped, folds and stacking membrane structures also can be found at the surface of the SCC hydrogel, it should be the structure from double-network hydrogel, as shown in the image which was amplified locally at up right. The images from SC and CaCS hydrogel show in Figs. S1a and b (Supporting information). It can be found from the images that fusiform structures can be observed from SC solution and folded structures appeared in the CaCS hydrogel. The chapped membrane from double-network hydrogel can provide tension properties to prevent the rupture of the hydrogel membrane along with the skin movement, and large number of fusiform from CMC can absorbed body fluid and reduced the exudate of body fluid. As show in Fig. 1c, once sodium alginate came into contacted with calcium ion, the sodium ion connected with the hydroxyl surface is replaced by calcium ion rapidly, forming an eggshell like structure [18]. The structure takes calcium ion as the cross-linking point and the molecular chain of sodium alginate is on it. In addition, the hydroxyl group on the surface of sodium alginate and the amino group on the molecular chain of chitosan are entangled on the surface of calcium ion and sodium alginate by intermolecular electrostatic adsorption, which makes the structure of the system more solid. In addition, when the pH decreased, CMC sodium folded, change the crosslinking degree of hydrogel and improve the mechanical property of the double-network hydrogel [19,20].

The addition of ethanol can stabilize the solution of chitosan and calcium chloride. Fig. 1d exhibits the FT-IR spectra of different hydrogel samples. The characteristic peaks of CMC at about 2829 cm^{-1}, 1608 cm^{-1} and 1359 cm^{-1} are attributed to asymmetric stretching vibration of $-CH_2$, stretching vibration of C = O and stretching vibration of C–O, the characteristic peak at 1407 cm^{-1} for stretching vibration of COO– on samples [21,22]. The characteristic peak at 2827 cm^{-1} and 1608 cm^{-1} ascribe to asymmetric stretching vibration of $-CH_2$ and COO– asymmetric stretching vibrations on sodium alginate. The absorption peak at 1410 cm^{-1} may be assigned to C–OH deformation vibrations with contribution of COO– symmetric stretching vibrations of carboxylate group. The other two weak peaks, with the peak center at approximately 1110 cm^{-1} and 1032 cm^{-1} may be attributed to C–C stretching vibration of pyranose rings and C–O stretching vibrations [23–25]. The FT-IR peaks of chitosan at 1598 cm^{-1} and 1090 cm^{-1} were attributed to N–H stretching vibration with amide II band and skeletal vibration involving the bridge C–O stretch of glucosamine [26]. After forming hydrogel membrane, the FT-IR spectrum of hydrogel shows characteristic other peak at 870 cm^{-1} attributed to vibration peak of out of plane CO_3^{2-} deformation, which due to sodium alginate processed carbonic acid and reaction with calcium ion to form calcium chelate. After forming membrane, strength peak of SCC hydrogel at 1608 cm^{-1} was weaker than another sample and the peak at 1401 cm^{-1} even disappeared, which indicated that the alginate and chitosan have been reacted to form hydrogel. All these results showed the SCC hydrogels membrane was successfully synthesized.

The rheological properties of hydrogels are evaluated according to the storage modulus (G') and the loss modulus (G"). Therefore, we used the rheometer equipment to test the performance characteristics of CMC/CaCS, SA/CaCS and SCC hydrogels at the fixed frequency (1 rad/s) [27]. The rheological measurement showed that the storage modulus of each sample was higher than the loss modulus, which indicated that the composite materials successfully changed from the colloidal state to the gel state [23]. However, differences among the three hydrogel samples were obvious. In order to observe the strength of hydrogel film from different raw materials, we first put the glass plate in the angle of 30° with horizontal plane, and then CMC, SA and SC solution were dropped on the sur-

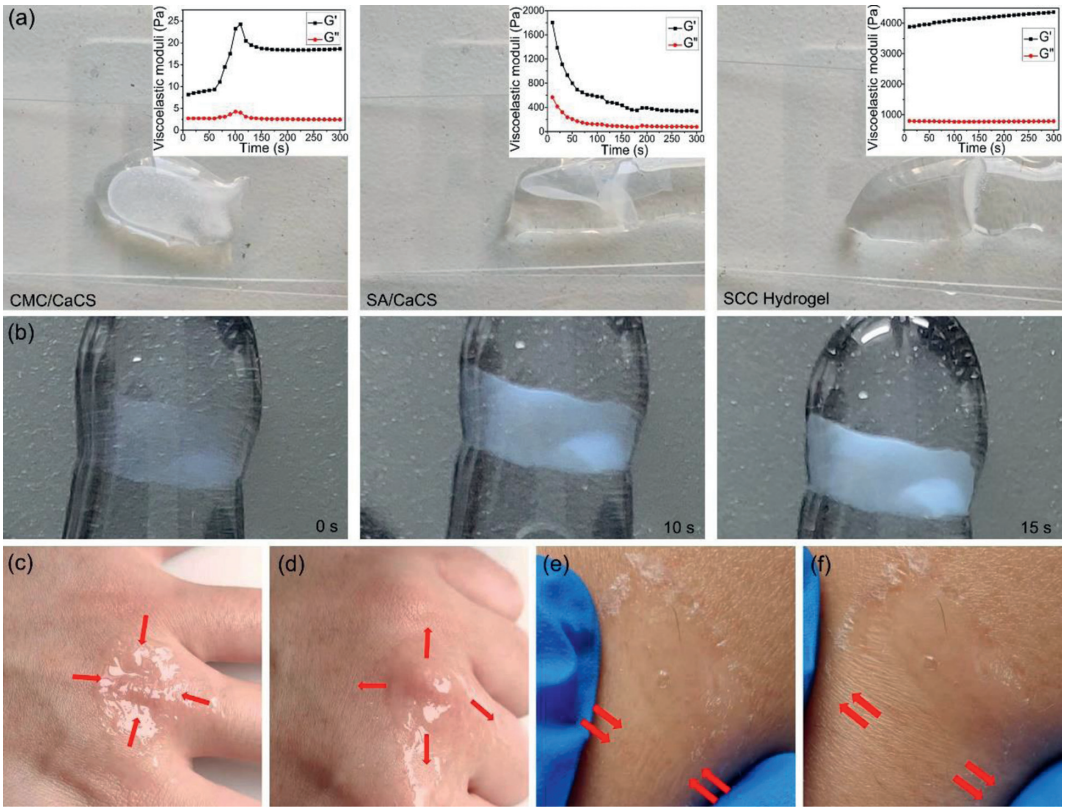

Fig. 2. (a) the rheology moduli of CMC/CaCS, SA/CaCS and SCC hydrogel from left to right, in 5 min (The left, middle and right inset represent the hydrogel rheological property of CMC/CaCS, SA/CaCS and SCC hydrogel.); (b) The film forming speed test of SCC hydrogel; (c) the SCC hydrogel contract under moisture condition; (d) the SCC hydrogel stretches under moisture condition; (e) the SCC hydrogel contract under dry condition; (f) the SCC hydrogel stretches under dry condition.

face of the substrate respectively, then CaCS were dropped to form hydrogel. As show in the left of Fig. 2a, the storage modulus and loss modulus of CMC/CaCS hydrogel were several orders of magnitude lower than those of the other two kinds of hydrogels, indicating that the rigidity of the materials after mixing was poor and unable to match the skin moving. The embedded picture displayed that CaCS contacted with CMC solution to form a membrane, but this membrane unable to support the gravity of CaCS solution, then solution CaCS continued to flow downward to form a soft concave film. A lot of white particles appeared on surface of CMC/CaCS hydrogel film. This is due to the fact that CMC chain contains a lot of hydroxyl groups. The CMC chain was turned to loosen under the neutral or alkaline condition. When the environment is filled with a large amount of Lewis acid, the molecular chain of CMC begins to contract and agglomerate. Therefore, the CMC solution is not only physical crosslinking with chitosan, but also agglomeration due to the change of surrounding pH [19,28,29].

As shown in the middle image of Fig. 2a, the Young's modulus of SA/CaCS hydrogel film that form in the same condition can be found higher than CMC/CaCS hydrogel. The insert-pictures showed that the CaCS solution still entered SA solution to form wrinkle structure, which illustrated that the two solutions reacted in contact interface and formed a membrane. Yet the membrane strength was not enough, which was broken by the CaCS solution and led to the formation of a new membrane again after a while. Rheological property of SA/CaCS hydrogel was shown in the middle insert image of Fig. 2a. At room temperature, the rheological properties of SA/CaCS hydrogel indicated that the young modulus was high when the gel was formed at room temperature, indicating that the hydrogel has certain mechanical strength at the beginning. However, the G' and G" of SA/CaCS hydrogel decreased in the first 200 s and then it can be found stabilized with time increasing. Results illuminated that the hydrogel formed by SA and CMC was gradually hydrolysis. According to the previous literature, we can see that the elasticity of the gel is directly related to the number of mesh points in the network [30,31]. When the calcium ions according to the influence of ions diffusion mechanism reacting with α-L-gluronie of alginate, the solution changed from sol to gel. In the gel forming processing, the calcium concentration in solution continuously decreased until it less than the sodium ions concentration. Beside the balance point, the sodium ions began to substitute for calcium ions on mesh points in hydrogel until the concentrations of two ions were equal, which results that the G' and G" of hydrogel decreasing until stable [32].

The insertion diagram on the far right of Fig. 2 shows the SCC hydrogel film able to withstand the same liquid quality without rupture. The rheological behavior of SCC hydrogel showed that the storage modulus and loss modulus of SCC hydrogel were higher, indicating that the hydrogel had good mechanical properties. The reasons for the high strength of the hydrogel were superimposed factor of the "egg-box" structure from calcium ions /alginate and electrical absorbed between CMC and chitosan [33,34]. More importantly, the CMC monomer was probable introduced into the "egg-box" structure. In the reaction process, the CMC monomer electrostatic adsorbed with chitosan on "egg-box" structure like alginate to form a stable outer layer. This outer layer can prevent sodium ions to replace calcium ions to keep a certain mechanical strength, thereby enhancing the rigidity of hydrogels.

To further showing the film-forming velocity, we observed the interactions and reactions between SC and CaCS solution as shown in the picture of Fig. 2b. Hydrogel film transformation from the transparent to translucent is visible by the naked eye. When SC and CaCS solution attached with each other at 0 s, a translucent thin film can be found at the interface. At 10 s, a white film was

formed, and the film can be found a glowing appearance when light is passing through it. At 15 s, a nontransparent white film was formed with a stable morphology, which can be seen from the experiments that the gel is fast forming with a stable morphology. The formation speed of hydrogel was mainly affected by the diffusion rate of calcium ions, which accords with the kinetics law of gel. Therefore, when calcium ions contact with sodium alginate, the hydrogel formed completed instantaneously, as the phenomena we observed [35].

Besides, we observed the formation process of hydrogels by confocal microscopy, as shown in Fig. S2 (Supporting information). Firstly, CaCS solution was added to the glass slide (0 s), and then SC solution dyed with rhodamine B was added on the top of the glass slide. It can be observed that in the gel, rhodamine B (excitation wavelength 488 nm) shows strong red light in CaCS solution, and the direction of diffusion is from bottom to top. After adding the CaCS droplets, the two solutions cross-linked rapidly to form a thin film with red color changing from inside to outside. Besides this phenomenon, the blank area increased significantly. Above results showed that when the solution mixed with each other, the original solution contracted and formed a hydrogel membrane, it tightly attached to the surface. Based on this phenomenon, we further studied on adhesion ability of hydrogels on skin to verify adhesion performance of SCC hydrogel.

Moreover, we designed a series of experiments to test the adhesion ability of hydrogels on skin when it was dry and moisture. Under wet condition, both compression and stretch properties of hydrogel showed excellent mechanical properties, which is followed by large deformation of the skin, as shown in Figs. 2c and d. Similarly, in a dry state, the hydrogel also attached the skin without affecting of the membrane structure, as shown in Figs. 2e and f. The results showed that with spray the SCC hydrogel onto skin, it exhibits particularly good adhesives and compatibility with skin, excellent attachment and painless removal properties also can be observed including in both dry and excess moisture conditions. As show in the results, it was found that SCC film was conformal attached on human skin and deform as the body moves. The excellent adhesion property of hydrogel is due to the presence of a large number of oxygen-containing groups on its surface, such as, carboxyl and hydroxyl groups on the surface of hydrogels. The oxygen-containing groups are able to form hydrogen bonds with water molecules on the surface of mammalian skin, so the hydrogel can be affixed to skin and move with it.

In order to investigate the influence of skin surface after attached by SCC hydrogel, we test skin statement by Courage + Khazaka electronic GmbH equipment, as shown in Fig. S3a (Supporting information). Levels of skin sensitive, skin moisture, sebum, pigmentation and wrinkle were quantified, from the results we can find that after the treatment of SCC hydrogel, skin was kept well, skin moisture increased and sebum of skin dropped off, we decided from the results that, the hydrogel have a good protection effect for trans-epidermal water loss. Beside these results, pigmentation and appearance of wrinkle of the skin turn to reduction [36]. At least in four hours, the film with excellent durability effectively improves the motion of skin, and reduces the appearance of skin wrinkles, as shown in Figs. S3b and c (Supporting information).

In order to protecting wound tissue from injury, wound healing dressings are more attractive due to their excellent antibacterial properties [32]. Agar was used as culture medium, and *Escherichia coli* was coated on the Petri dish. After incubation for 48 h, the agar medium was staining by DAPI, and the control group was full on the Petri dish, as shown in Fig. S4a (Supporting information). Fig. S4c (Supporting information) shows that after fluorescent staining, the control group was full colony of *E. coli*, but the SCC hydrogel group was disappeared. *E. coli* is very difficult to be eliminated or killed, since its complex cell wall. However, under confocal microscope, as showed in Fig. S4d (Supporting information), *E. coli* can be hardly found in the SCC hydrogel group illuminated the excellent sterilization effect of SCC hydrogels [37]. This phenomenon indicates that the prepared membrane has good antibacterial ability, which due to the positive-changed groups of SCC hydrogel could damage the walls of the bacteria by electrostatic adherence with cytoderm of bacteria, leading the intracellular fluids release to kill bacteria [38]. The results of antibacterial experiments illustrated that SCC hydrogel membrane with good antibacterial properties.

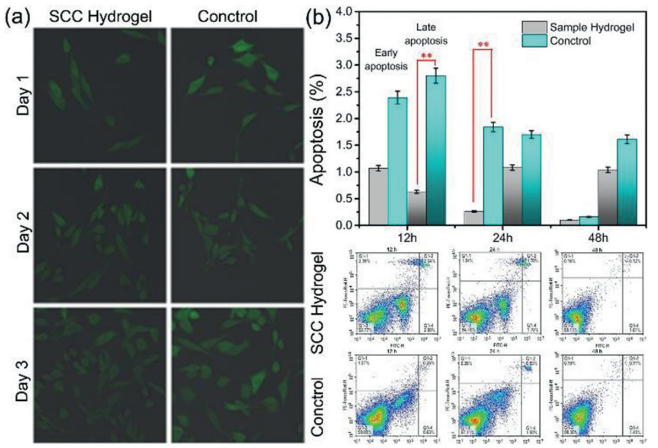

Fig. 3. (a) Cell (cultured on SCC hydrogel or in six-well dishes) morphology. (b) Cells flow cytometry analysis for apoptosis detection ($^{**}P < 0.01$) among the indicated groups.

Fig. 3a show the growth speed of the cells in different environment, as show in the image, cells were in a high density on SCC hydrogel, with good cell morphology. In control group, cells are also growing well but the density of the cell was lower than the ones on SCC hydrogel. In conclusion, we contrast the shape and adhesion of the cells on SCC hydrogel and in 6-well dishes, the results show that cells grow better on the hydrogel.

Cell apoptosis assay from 12 h to 48 h was conducted *via* flow cytometry showing in Fig. 3b. The cells cultured in the 6-well dishes was set as control group, show in blue columnar in the image and the ones cultured on SCC hydrogel show in gray columnar. According to the results, compare with the cells on SCC hydrogel, much more quantities cells in control group show late apoptosis and severe cell necrosis at the first 12 h. In 24 h, cell necrosis and early apoptosis of cells can be found obviously high in the control group compared with the SCC group ($P < 0.01$). After 48 h, both of groups were show inhibits in early and late apoptosis, cells in control groups still show much serious in apoptosis while necrosis increased rapidly.

The Fig. 4a indicates a schematic diagram of wound healing in mice treated with hydrogel dressing. Spray the SC solution onto the wound surface of mice, then spray the CaCS solution onto the wound, and spray it once a day. In the animal model, the wound with a diameter of 20 mm was created on the dorsal area of Sprague Dawley rats. The SCC hydrogel and commercialized wound dresses were used to cure two different groups. We contrasted the two groups with their wound area contracted on days 0, 1, 3, 7, 17, 21 as shown in Fig. 4b. It can be found that the changes of the wounds were not obviously in both of groups at the first day with therapy. However, the amount of blood exudation in SCC group was significantly less than that in market group. Until the third day, the heal area was significantly different. Specifically speaking, we found that with 3 days therapy, hydrogel groups reduce the wound area to 80.5% ± 6.1%, and for the control group (marketing), it took 7 days to reduce the wound area to 75.6% ± 3.4%. This

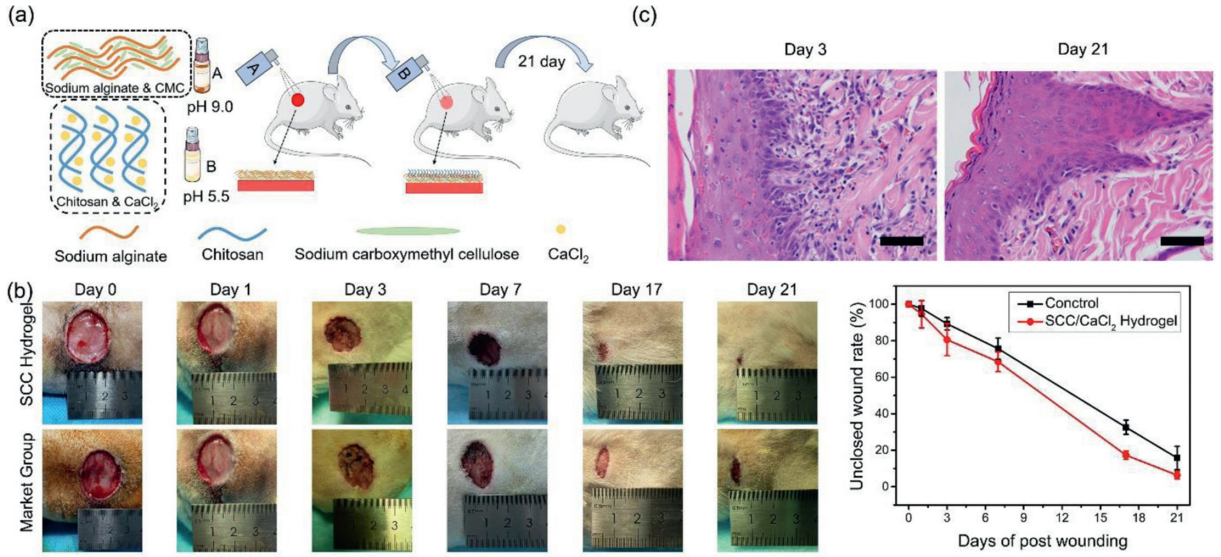

Fig. 4. Wound healing progress: (a) Schematic diagram of hydrogel for wound healing in mice; (b) Gross observation of the heal *in vivo* during different periods, quantitative statistical analysis of wounds closure for market group and SCC hydrogel; (c) Haemotoxylin and eosin (H&E) staining of wounds at day 3 and day 21 (scale bar: 20 μm).

result demonstrated SCC hydrogel comparatively higher promotion effect on wound healing. After 17 days of treatment, the size of wound area was found to be 17.2% ± 2.3% in the hydrogel group, at this time point, the wound area of control group was found to be 32.5% ± 3.9%. There was a small block wound in the hydrogel group present on day 21, which is obviously better than the wound treated with commercial wound healing dressings.

From the results it can be found when treated with SCC hydrogel the wound healing speed was faster than the ones treated with market products. We suggest the effects of SCC hydrogels are associated with two important components: alginate and chitosan. Alginate can trigger macrophages to produce tumor necrosis factor (TNF-α), which can lead to increase of inflammatory signals that result in macrophage activity, level of cytokines in the wound will increased and speed up the wound healing process [39]. In addition, chitosan can promote the migration of polymorphonuclear neutrophils, promote granulation proliferation and induce dermal fibroblasts [40,41]. Haemotoxylin and eosin (H&E) staining were applied to further investigate the wound healing of SCC hydrogel on rats. Fig. 4c displays the histological results of the wounds in market group and SCC hydrogel group on postoperative day 21, respectively. As shown in the representative images of H&E-stained wound, the cross section of wound treated with market group is irregular, indicates that the wound is still in the healing process. In SCC hydrogel group, the wound showed more densely packed collagen fibers with parallel arrangement, more mature cells with the color of deep purple can be found, as show in the image. We deduced from the results that, wound in the SCC hydrogel group exhibit rapid skin regeneration and lighter scars can be expected.

In this study, we successfully formed double-network hydrogels by spray method from polymer-based multi-ionic liquids. The double-network hydrogel was rapidly formed from cross and simultaneous polymerization from different polymers. The hydrogels show better biocompatibility and broad commercial prospects in the field of wound dressing. It will be much simple and convenient in clinical application. As the main material of hydrogel, degree of deacetylation determined the properties of chitosan, much importantly, the chitosan also has a high capacity for entrapping various ions including (Ca^{2+}, Mg^{2+}, Zn^{2+}) under acidic condition, which is advantage to the double-network hydrogel synthesized from chitosan and alginate [12].

Another material alginate is composed of a block of (1,4)-linked β-D-mannuronate (M) and α-L-guluronate (G) residues, and sequence of M and G residues determine the alginate physical properties and molecular weight, such as formed hydrogel by divalent cation [13]. In particular, capturing divalent ion is directly dependent on the amount of G-block present in the alginate structure [14]. The addition of G fragments is beneficial to improving the weak mechanical strength and weak water storage capacity of alginate gel [42]. However, it is not enough to rely only on the chelation of calcium ion and alginate and the electrostatic adsorption of alginate and chitosan, which will reduce the link point with the decrease of water content and the increase of sodium ion content [32]. We add an anionic water-soluble material, carboxymethyl cellulose sodium, to increase the strength of hydrogel junction while reducing the cost.

This type of hydrogel including pH sensitivity, forming rapidly network hydrogel by sodium alginate intercepting calcium ion and weave on this structure CMC and chitosan to prevent bleeding spray can used to treat skin wound healing as wound dressing. With the property of rapid film formation and adhesive on the wound surface, the hydrogel can also prevent bacterial invasion and repair the wound, this type of double-network hydrogel can be chosen for latest generation of wound dressing. Based on the simple steps of the preparation process and convenient operation for application, this hydrogel had broad market prospects for less deduction.

Declaration of competing interest

There are no conflicts to declare.

Acknowledgments

We thank for the funding supports from SceneRay. This research is supported by the National Natural Science Foundation of China (No. 11204033), CMA L'Oreal China Skin Grant 2015 (No. S2015121421) and the Open Research Fund of State Key Laboratory of Natural Medicines, China Pharmaceutical University (No. SKLNMKF201803), Southeast University Institution Basal Research Fund.

Supplementary materials

Supplementary material associated with this article can be found, in the online version, at doi:10.1016/j.cclet.2021.11.047.

References

[1] A. Moeini, P. Pedram, P. Makvandi, M. Malinconico, G.G. d'ayala, Carbohyd. Polym. 233 (2020) 16.
[2] A. Sun, X.Y. He, L. Li, et al., Npg Asia Mater. 12 (2020) 1.
[3] X.H. Chen, P.F. Tan, Y. Wen, et al., Chin. Chem. Lett. 31 (2020) 1499–1503.
[4] C.H. Xian, Z.P. Gu, G.T. Liu, J. Wu, Chin. Chem. Lett. 31 (2020) 1612–1615.
[5] P.G. Jian, Soft Matter. 12 (2010) 6.
[6] E.S. Dragan, Chem. Eng. J. 243 (2014) 572–590.
[7] Y.X. He, Y. Li. D. Sun, et al., Carbohydr. Polym. 261 (2021) 11.
[8] H.P. Si, T.L. Xing, Y.L. Ding, et al., Polymers (Basel) 11 (2019) 21.
[9] X.Y. He, A. Sun, T. Li, et al., Carbohydr. Polym. 247 (2020) 116692.
[10] H. Hamedi, S. Moradi, S.M. Hudson, et al., Carbohydr. Polym. 199 (2018) 445–460.
[11] R. De Souza, P. Zahedi, C.J. Allen, M. Piquette-Miller, Biomaterials 30 (2009) 3818–3824.
[12] K. Kurita, Polym. Degrad. Stabil. 59 (1998) 117–120.
[13] S.H. Ching, N. Bansal, B. Bhandari, Crit. Rev. Food Sci. 57 (2017) 1133–1152.
[14] B.L. Strand, Y.A. Morch, G. Skjak-Braek, Minerva. Biotecnol. 12 (2000) 223–233.
[15] X.D. Chen, Small Methods 1 (2017) 4.
[16] M. Yadollahi, I. Gholamali, H. Namazi, M. Aghazadeh, Int. J. Biol. Macromol. 73 (2015) 109–114.
[17] B.L. Guo, J.F. Yuan, Q.Y. Gao, Int. Polym. Proc. 57 (2008) 463–468.
[18] S. Venkataraman, J.L. Hedrick, Z.Y. Ong, et al., Adv. Drug. Deliver Rev. 62 (2011) 1228–1246.
[19] O.S. Lawal, M. Yoshimura, R. Fukae, K. Nishinari, Colloid. Polym. Sci. 289 (2011) 1261–1272.
[20] S.P. Yang, S.Y. Fu, Y.M. Zhou, C.L. Xie, X.Y. Li, Int. J. Polym. Mater. 60 (2011) 62–74.
[21] H.S. El-Sayed, S.M. El-Sayed, A.M.M. Mabrouk, G.A. Nawwar, A.M. Youssef, J. Polym. Environ. 29 (2021) 1941–1953.
[22] J.H. Ning, X. Luo, F.X. Wang, et al., Sensors 19 (2019) 17.
[23] T.T. Wu, J.Q. Huang, Y.Y. Jiang, et al., Food Chem. 240 (2018) 361–369.
[24] W. Yue, H.H. Zhang, Z.N. Yang, Y. Xie, Carbohydr. Polym. 251 (2021) 117104.
[25] X.X. Li, A.H. Xu, H.G. Xie, et al., Carbohydr. Polym. 79 (2010) 660–664.
[26] D. Archana, B.K. Singh, J. Dutta, P.K. Dutta, Int. J. Biol. Macromol. 73 (2015) 49–57.
[27] W.J. Huang, Y.X. Wang, Z.Q. Huang, et al., ACS Appl. Mater. Interfaces 10 (2018) 41076–41088.
[28] W.B. Wang, J.X. Xu, A.Q. Wang, Express Polym. Lett. 5 (2011) 385–400.
[29] P.V. Kulkarni. Kulkarni, J. Keshavayya, V.H. Kulkarni, Polym. Advan. Technol. 18 (2007) 814–821.
[30] N.M. Velings, M.M. Mestdagh, Polym. Gels. Netw. 3 (1995) 311–330.
[31] T. Wang, G.W. Qu, C. Wang, et al., Langmuir 35 (2019) 13999–14006.
[32] C. Ouwerx, N. Velings, M.M. Mestdagh, Mav. Axelos, Polym. Gels & Netw. 6 (1998) 393–408.
[33] T.C. Tseng, L. Tao, F.Y. Hsieh, et al., Adv. Mater. 27 (2015) 3518–3524.
[34] T.G. Grant, E.R. Morris, D.A. Rees, P.J.C. Smith, D. Thom, FEBS Lett. 32 (1973) 195–198.
[35] D. Quong, R.J. Neufeld, G. Skjak-Bræk, D. Poncelet, Biotechnol. Bioeng. 57 (1998) 438–446.
[36] D. Gopinath, M.R. Ahmed, K. Gomathi, et al., Biomaterials 25 (2004) 1911–1917.
[37] C.Q. Qin, Q. Xiao, H.R. Li, et al., Int. J. Biol. Macromol. 34 (2004) 121–126.
[38] A.A. Menazea, M.M. Eid, M.K. Ahmed, Int. J. Biol. Macromol. 147 (2020) 194–199.
[39] D. Yang, K.S. Jones, J. Biomed. Mater. Res. A 90 (2009) 411–418.
[40] H. Ueno, H. Yamada, I. Tanaka, et al., Biomaterials 20 (1999) 1407–1414.
[41] G.I. Howling, P.W. Dettmar, P.A. Goddard, et al., Biomaterials 22 (2001) 2959–2966.
[42] E.A. Kamoun, E-R.S. Kenawy, X. Chen, J. Adv. Res. 8 (2017) 217–233.